

Frequency and Time Domain Analysis of Influence of the Grounding Electrode Conductivity on Induced Current Distribution

Silvestar Šesnić, and Dragan Poljak

Original scientific paper

Abstract—The paper deals with an assessment of the influence of finite conductivity to the current induced along the horizontal grounding electrode. Analysis is performed in frequency and time domain, respectively. Current distribution along the grounding electrode buried in a lossy half-space is determined via analytical solution of the corresponding Pocklington equation in the frequency domain. The corresponding time domain response is obtained by means of Inverse Fast Fourier Transform (IFFT). The electrode is excited via an equivalent current source. Presence of the earth-air interface is taken into account via the simplified reflection coefficient arising from the Modified Image Theory (MIT). The electrode current is calculated for the case of perfectly conducting (PEC) electrode and for the electrodes made of copper and aluminum. Comparison of results shows no significant discrepancy between these electrodes, justifying the use of a PEC electrode approximation.

Index Terms—Grounding electrode, finite conductivity, induced current, analytical solution

I. INTRODUCTION

DESIGN of an adequate lightning protection system (LPS) is one of primary concerns in the field of wind power generation. Since wind turbines are very susceptible to lightning strikes, the appropriate model of a LPS is necessary [1]–[3]. The horizontal electrode is a fundamental part of almost every grounding system and its model represents a starting point in the analysis of more complex structures. The current induced along the electrode is a basic parameter in the electromagnetic analysis of the grounding systems [4]. Grounding electrodes are usually made of copper or aluminum [5], so it is important to determine the influence of the material

conductivity on the induced current distribution, since introduction of this parameter further complicates the model and subsequent calculations.

Transient current induced along the grounding electrode, represented as a thin wire, can be obtained using direct or indirect approach. Direct approach implies modeling of the electromagnetic coupling to thin wire directly in time domain [6]. The indirect approach, used in this paper, implies formulation and solution in the frequency domain, where time domain solution is obtained using certain inverse transform procedures [6], [7].

Current induced along the grounding electrode is governed by some variant of integral or integro-differential equation (Hallen or Pocklington type), respectively. Solution of these equations is, in most cases, undertaken using numerical methods. On the other hand, analytical solution can be obtained when dealing with canonical problems [8]–[10]. Analytical solutions, as opposed to numerical ones, can be used for quick estimation of the observed phenomenon. Valuable contributions in the area of analytical solutions of integral equations in the antenna theory are given by R. W. P. King *et al.* [11]–[14] who gave expressions for different parameters of the antenna, primarily in the frequency domain. The analytical solution for the current induced along the grounding electrode in the frequency domain has been reported by the authors in [15].

In section II, a Pocklington integro-differential equation for the current induced along the grounding electrode buried into a lossy half-space, excited with an equivalent current source is derived. The influence of the earth-air interface is taken into account via simplified reflection coefficient arising from the Modified Image Theory (MIT). In section III, the analytical solution of the corresponding Pocklington equation is given and the influence of the electrode conductivity is clarified. Section IV contains comparison of numerical results for the current distribution along the perfectly conducting (PEC) electrode and the electrodes with finite conductivity.

II. ANTENNA OF A GROUNDING ELECTRODE

Grounding electrode of length L and radius a is horizontally buried at depth d into a lossy medium with electrical permittivity ϵ and conductivity σ , as shown in Figure 1.

Manuscript received December 6, 2012; revised June 6, 2013. The material in this paper was presented in part at the 20th International Conference on Software, Telecommunications and Computer Networks (*SoftCOM 2012*), Split, Croatia, Sept. 11–13, 2012.

S. Šesnić is with the Department of Power Engineering, University of Split, Split, Croatia (phone: +385-21-305-814; fax: +385-21-305-776; e-mail: ssesnic@fesb.hr).

D. Poljak is with the Department of Electronics, University of Split, Split, Croatia (e-mail: dpoljak@fesb.hr).

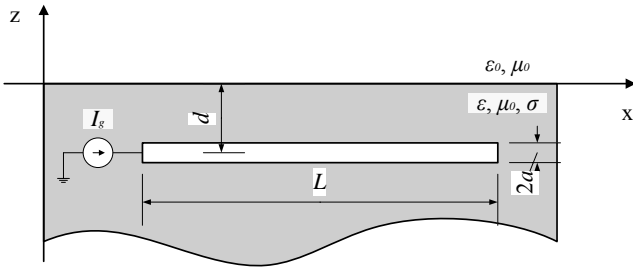


Fig. 1. Horizontal grounding electrode.

Grounding electrode is excited with an equivalent current source representing a lightning strike current. Governing equation for the current induced along the electrode can be derived by imposing the continuity condition for the tangential component of the total electric field, being expressed as a sum of the incident \vec{E}^{inc} and scattered field \vec{E}^{sc} , at the surface of the electrode [4], [15]

$$\vec{e}_x \cdot (\vec{E}^{inc} + \vec{E}^{sc}) = Z_L(\omega) I(x), \quad (1)$$

where $I(x)$ represents current induced along the electrode and $Z_L(\omega)$ internal per-unit-length impedance of the electrode given as [16]

$$Z_L(\omega) = \frac{1}{2\pi a} \sqrt{\frac{j\omega\mu_0}{\sigma_w + j\omega\epsilon_w}} \frac{I_0(\gamma_w a)}{I_1(\gamma_w a)}, \quad (2)$$

where ϵ_w and σ_w represent permittivity and conductivity of the electrode, respectively, and γ_w is propagation constant of the material given with

$$\gamma_w = \sqrt{j\omega\mu_0\sigma_w - \omega^2\mu_0\epsilon_w}. \quad (3)$$

$I_0(\gamma_w a)$ and $I_1(\gamma_w a)$ are modified Bessel functions of zero and first order, respectively, with complex argument $\gamma_w a$.

In case of high conductivity material, when $\sigma_w \gg 2\pi f\epsilon_w$, internal impedance (2) can be written as [16]

$$Z_L(\omega) = \frac{1}{2\pi a} \sqrt{\frac{j\omega\mu_0}{\sigma_w}} \frac{J_0(\gamma_w a)}{J_1(\gamma_w a)}, \quad (4)$$

where $J_0(\gamma_w a)$ and $J_1(\gamma_w a)$ represent Bessel functions of zero and first order, respectively. Propagation constant can be expressed with [16]

$$\gamma_w = \sqrt{j\omega\mu_0\sigma_w}. \quad (5)$$

Furthermore, taking into account the thin wire approximation, the axial component of a scattered field can be expressed in terms of magnetic vector and electric scalar potential, as [7], [17]

$$E_x^{sc} = -j\omega A_x - \frac{\partial\phi}{\partial x}. \quad (6)$$

Vector and scalar potentials are given by particular integrals

$$A_x = \frac{\mu}{4\pi} \int_0^L I(x') g(x, x') dx', \quad (7)$$

$$\phi = \frac{1}{4\pi\epsilon_{eff}} \int_0^L q(x') g(x, x') dx', \quad (8)$$

where $q(x')$ denotes charge distribution along the electrode.

Complex permittivity of the medium is given with

$$\epsilon_{eff} = \epsilon - j\frac{\sigma}{\omega}. \quad (9)$$

Green's function $g(x, x')$ can be expressed in terms of [18]

$$g(x, x') = g_0(x, x') - \Gamma_{ref} g_i(x, x'), \quad (10)$$

where $g_0(x, x')$ denotes the lossy medium Green's function

$$g_0(x, x') = \frac{e^{-\gamma R_1}}{R_1} \quad (11)$$

and $g_i(x, x')$ is a Green's function according to the image theory

$$g_i(x, x') = \frac{e^{-\gamma R_2}}{R_2}. \quad (12)$$

Propagation constant of the medium is defined as

$$\gamma = \sqrt{j\omega\mu\sigma - \omega^2\mu\epsilon}. \quad (13)$$

and distances R_1 and R_2 correspond to distances from the source and the image to the observation point, respectively

$$R_1 = \sqrt{(x-x')^2 + a^2} \quad (14)$$

$$R_2 = \sqrt{(x-x')^2 + 4d^2}$$

Influence of the earth-air interface can be taken into account via the Sommerfeld theory involving analytically unsolvable integrals [19]. Simpler approximation involves an application of the Fresnel reflection coefficients, which ensures accuracy within 10% of the results obtained using rigorous Sommerfeld theory [20], [21]. However, in this paper, the influence of the interface is taken into account via the reflection coefficient arising from the Modified Image Theory and is given as [22]

$$\Gamma_{ref}^{MIT} = -\frac{\epsilon_{eff} - \epsilon_0}{\epsilon_{eff} + \epsilon_0}. \quad (15)$$

The validity of this approach has been thoroughly investigated in [23].

Since the grounding electrode is excited via equivalent current source, the incident electric field is equal to zero. Taking into account (1) and (6)–(8), the following integro-differential equation is obtained

$$j\omega \frac{\mu_0}{4\pi} \int_0^L I(x') g(x, x') dx' - \frac{1}{j4\pi\omega\epsilon_{eff}} \frac{\partial}{\partial x} \int_0^L \frac{\partial I(x')}{\partial x'} g(x, x') dx' + Z_L(\omega) I(x) = 0 \quad (16)$$

Equation (16) represents governing Pocklington integro-differential equation in the frequency domain for the current distribution along the horizontal electrode.

III. ANALYTICAL SOLUTION FOR THE INDUCED CURRENT

The current distribution along the electrode is obtained as solution of (16) by implementing an appropriate numerical method, e.g. Galerkin-Bubnov Boundary Element Method (GB-IBEM) as reported in [18]. However, an analytical solution can be derived using certain approximations. First, it is convenient to rewrite (16) in a following manner

$$-\frac{1}{j4\pi\omega\epsilon_{eff}}\left[\frac{\partial^2}{\partial x^2}-\gamma^2\right]\int_0^L I(x')g(x,x')dx' + Z_L(\omega)I(x) = 0 \quad (17)$$

which yields [15],[24]

$$\int_0^L I(x')g(x,x')dx' = I(x)\int_0^L g(x,x')dx' + \int_0^L [I(x')-I(x)]g(x,x')dx' \quad (18)$$

Second integral on the right hand side can be neglected and integral over Green's function approximated as follows[25]

$$\int_0^L g(x,x')dx' = 2\left(\ln\frac{L}{a}-\Gamma_{ref}^{MIT}\ln\frac{L}{2d}\right) = \Psi(\omega). \quad (19)$$

Approximation given in (18) partially neglects loss of energy due to radiation which can be significant for shorter electrodes (less than 1 m). However, in the medium with higher values of conductivity (around 10 mS/m), the dominant factor in the loss of energy is the conductivity of the medium itself, as the energy is dissipated primarily through the conduction and not radiation, so this approximation can be used.

Combining (17)–(19) leads to

$$\left[\frac{\partial^2}{\partial x^2}-\gamma^2-\frac{4\pi(j\omega\epsilon+\sigma)}{\Psi(\omega)}Z_L(\omega)\right]I(x,\omega) = 0. \quad (20)$$

The solution of differential equation (20) is readily given with [15]

$$I(x,\omega) = I_g(\omega)\frac{\sinh[\gamma_{eq}(L-x)]}{\sinh(\gamma_{eq}L)}, \quad (21)$$

where the equivalent propagation constant takes into account per-unit-length impedance of the electrode and is given as

$$\gamma_{eq}^2 = \gamma^2 + \frac{4\pi(j\omega\epsilon+\sigma)}{\Psi(\omega)}Z_L(\omega). \quad (22)$$

Current distribution described with (21) represents current induced along the grounding electrode in the frequency domain. It is important to point out that the equivalent propagation constant in the case of PEC electrode is equal to the propagation constant of the medium, since $Z_L(\omega) = 0$.

Equivalent current generator function is defined with $I_g(\omega)$ in the frequency domain. To obtain transient response to double exponential pulse excitation, which can be used to describe lightning strike current, its frequency domain counterpart is considered [18]

$$I_g(\omega) = I_0\left(\frac{1}{\alpha+j\omega}-\frac{1}{\beta+j\omega}\right). \quad (23)$$

Discrete frequency response is obtained by sampling (21) with

$$I(x,\omega_i) = \sum_{i=1}^N I(x,\omega)\delta(\omega-\omega_i). \quad (24)$$

Transient current induced at the center of the electrode is calculated using Inverse Fast Fourier Transform (IFFT) procedure by applying the following scheme

$$I(x,t_j) = \frac{1}{N}\sum_{i=1}^N I(x,\omega_i)\omega_N^{-(j-1)(i-1)}. \quad (25)$$

After extensive numerical testing, it has been found that optimal parameters for performing discrete sampling and subsequent IFFT include 2^{16} samples and maximum frequency of 500 MHz. When these parameters are considered, accurate results are obtained in a reasonable time frame.

IV. NUMERICAL RESULTS

In this section, some illustrative numerical examples are given. All calculations are performed for the grounding electrode of radius $a=5$ mm, buried at depth $d=1$ m into a lossy ground with relative permittivity $\epsilon_r=10$. The electrode conductivities are taken as the conductivities of the materials used for the grounding systems, namely copper ($\sigma_w=55$ MS/m) and aluminum ($\sigma_w=37$ MS/m) [5]. In addition, the calculations are made for the electrode of infinite conductivity. Electrode length, ground conductivity and the parameters of the current generator (frequency, pulse duration) are varied.

The first set of results, presented in Figures 2, 3, 4 and 5, shows comparison of the real and imaginary part of the induced current as well as absolute value of the current distribution along the electrode for different parameters of ground conductivity and source frequency. Magnitude of the current source at a given frequency is $I_g(\omega)=1A$, while length of the electrode is $L=10$ m. It can be seen that the values of current distribution for different electrode conductivities agree rather satisfactorily. Furthermore, current distribution for the electrode with extremely low conductivity $\sigma_w=370$ S/m is calculated to stress out the discrepancy of the results. In addition, it can be observed that the value of current monotonously falls from the current source to the end of the electrode at frequency $f=1$ MHz. On the other hand, at the frequency $f=10$ MHz, the oscillatory behavior of the current distribution is shown.

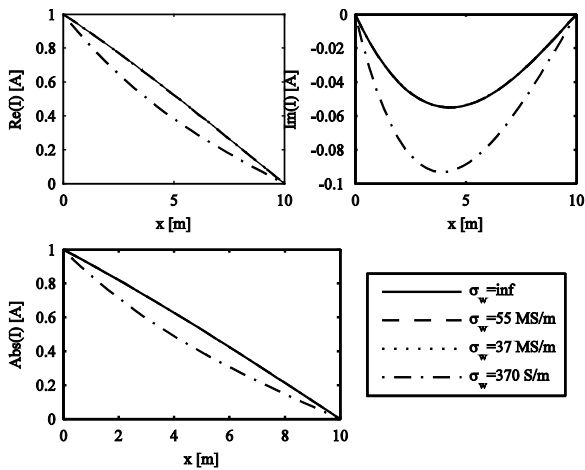


Fig. 2. Real, imaginary part and absolute value of the current induced along the electrode, $\sigma=1$ mS/m, $f=1$ MHz.

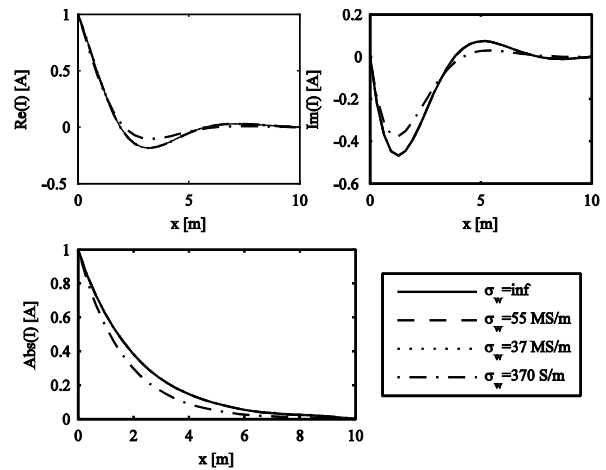


Fig. 5. Real, imaginary part and absolute value of the current induced along the electrode, $\sigma=10$ mS/m, $f=10$ MHz.

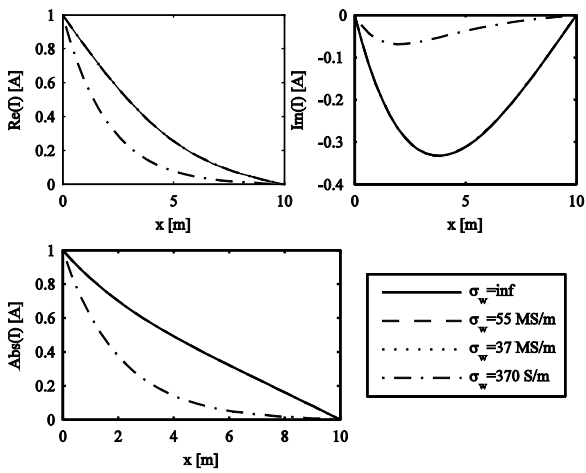


Fig. 3. Real, imaginary part and absolute value of the current induced along the electrode, $\sigma=10$ mS/m, $f=1$ MHz.

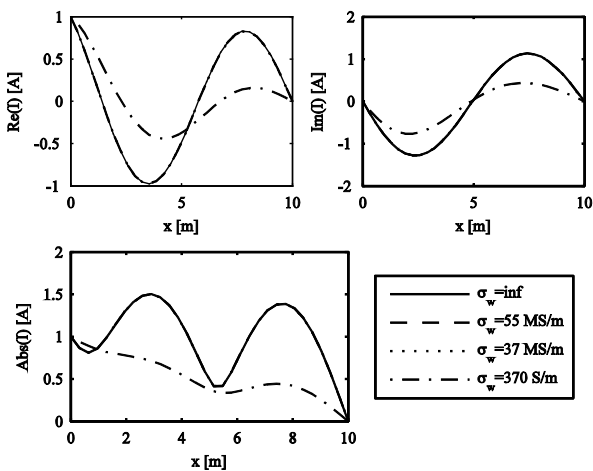


Fig. 4. Real, imaginary part and absolute value of the current induced along the electrode, $\sigma=1$ mS/m, $f=10$ MHz.

In addition, it is interesting to determine the frequency spectrum of the current induced at the center of the grounding electrode for various values of electrode length and ground conductivity. The set of results presented in Figures 6, 7, 8 and 9 show frequency spectrum of the absolute value of induced current. The results show no discrepancy between induced currents for various conductivities of the grounding electrode. The induced current along the electrode with extremely low conductivity, $\sigma_w=370$ S/m, is calculated to demonstrate the discrepancy.

As it can be seen from Figures 6 and 7, resonant frequency for electrode length $L=1$ m is around $f=50$ MHz and is almost independent of ground conductivity.

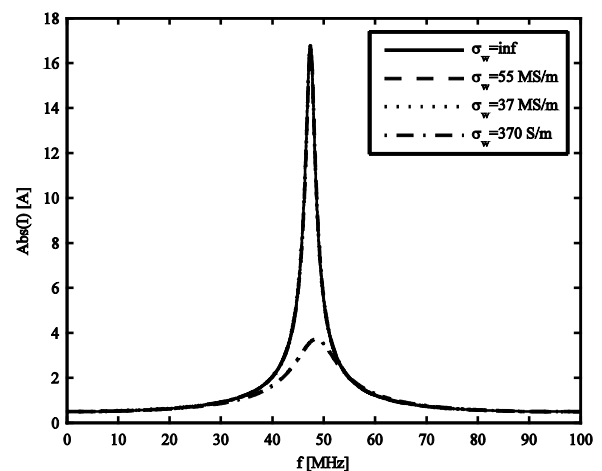


Fig. 6. Frequency spectrum of the current induced at the center of the grounding electrode, $L=1$ m, $\sigma=1$ mS/m.

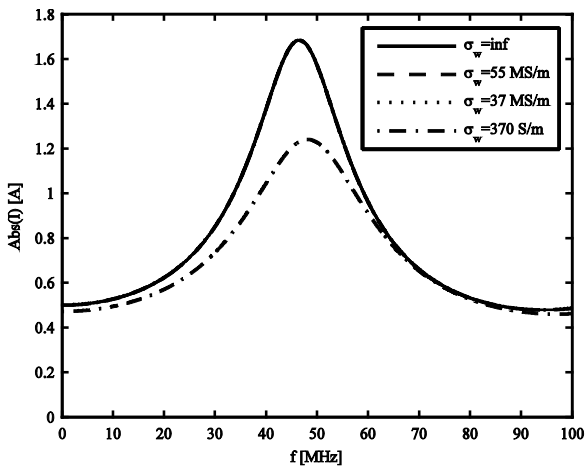


Fig. 7. Frequency spectrum of the current induced at the center of the grounding electrode, $L=1$ m, $\sigma=10$ mS/m.

On the other hand, Figures 8 and 9 show frequency spectrum for the electrode length $L=10$ m. For the ground conductivity $\sigma=1$ mS/m, resonant frequencies of the grounding electrode are observed to be odd multiplicities of $f=5$ MHz. However, Figure 9 shows no resonant frequency to exist for ground conductivity of $\sigma=10$ mS/m. This effect can be explained considering the denominator of (21).

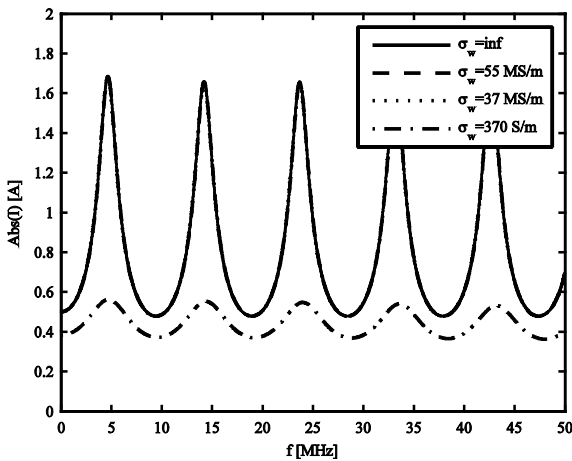


Fig. 8. Frequency spectrum of the current induced at the center of the grounding electrode, $L=10$ m, $\sigma=1$ mS/m.

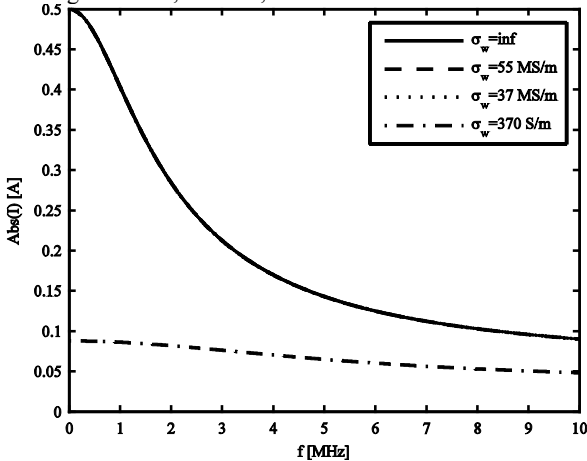


Fig. 9. Frequency spectrum of the current induced at the center of the grounding electrode, $L=10$ m, $\sigma=10$ mS/m.

Final computational examples take into account transient behavior of the current induced at the center of the grounding electrodes. The following set of results is calculated for the case of lightning pulse with parameters $\alpha=0.07924 \cdot 10^6$ 1/s and $\beta=4.0011 \cdot 10^6$ 1/s, which represent the $1/10 \mu\text{s}$ pulse [18]. The calculations are performed for the electrode length $L=1$ m and $L=10$ m, respectively and for the medium conductivity $\sigma=1$ mS/m and $\sigma=10$ mS/m, respectively. As it can be seen from Figures 10, 11 and 12, the results for the transient currents induced along the PEC electrode or the realistic electrodes, made of copper or aluminum, agree perfectly. An additional calculation has been done for the electrode with conductivity $\sigma_w=37$ S/m or $\sigma_w=370$ S/m to point out that for extremely low conducting materials the transient current differs.

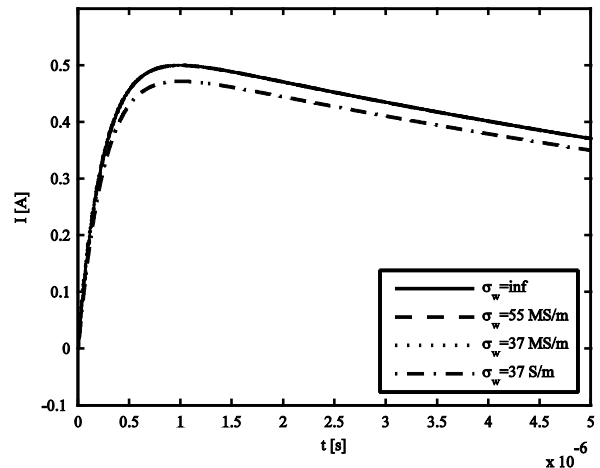


Fig. 10. Transient current at the center of the electrode, $L=1$ m, $\sigma=1$ mS/m, $1/10 \mu\text{s}$ pulse.

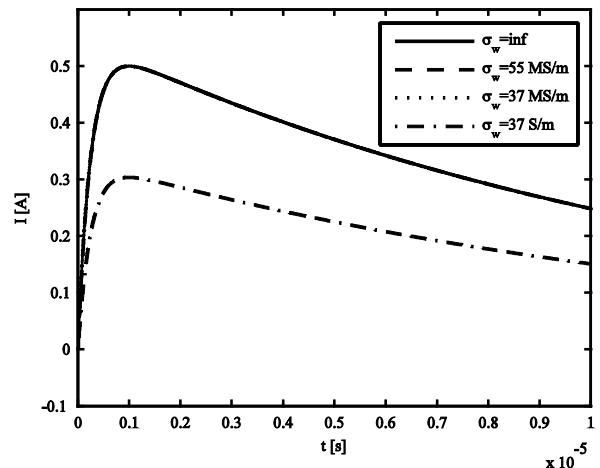


Fig. 11. Transient current at the center of the electrode, $L=1$ m, $\sigma=10$ mS/m, $1/10 \mu\text{s}$ pulse.

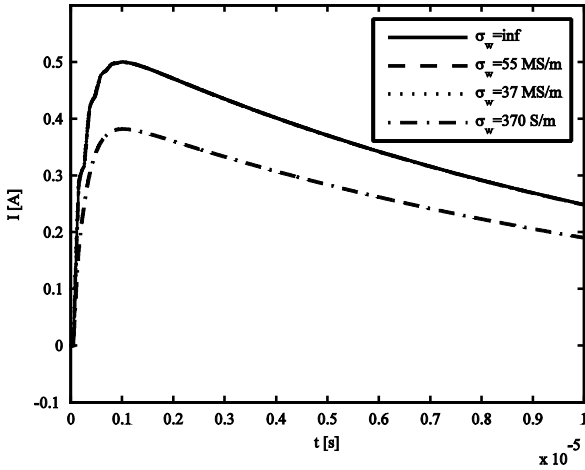


Fig. 12. Transient current at the center of the electrode, $L=10$ m, $\sigma=1$ mS/m, $1/10 \mu\text{s}$ pulse.

The following set of results, shown in Figures 13, 14, 15 and 16, are calculated for the current pulse with parameters $\alpha=0.07924 \cdot 10^7$ 1/s, and $\beta=4.0011 \cdot 10^7$ 1/s, which represent the $0.1/1 \mu\text{s}$ pulse. The length of the electrode is varied as $L=5$ m and $L=10$ m, respectively, while the conductivity of the medium is taken as $\sigma=1$ mS/m and $\sigma=10$ mS/m, respectively. The same, previously observed, behavior can be seen. The results for PEC electrode and realistic electrodes agree perfectly. The discrepancy can be seen only for extremely low conducting electrode with $\sigma_w=370$ S/m.

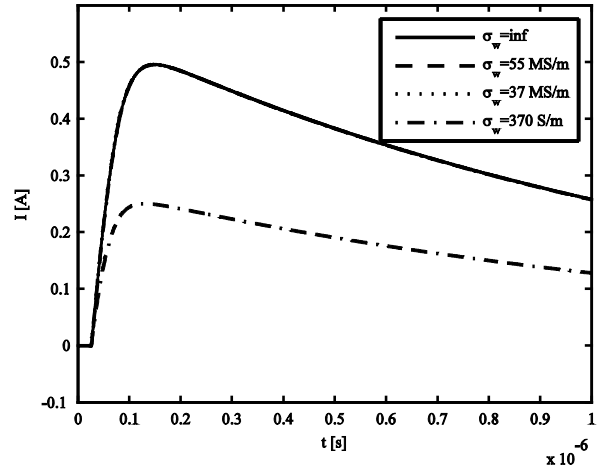


Fig. 14. Transient current at the center of the electrode, $L=5$ m, $\sigma=10$ mS/m, $0.1/1 \mu\text{s}$ pulse.

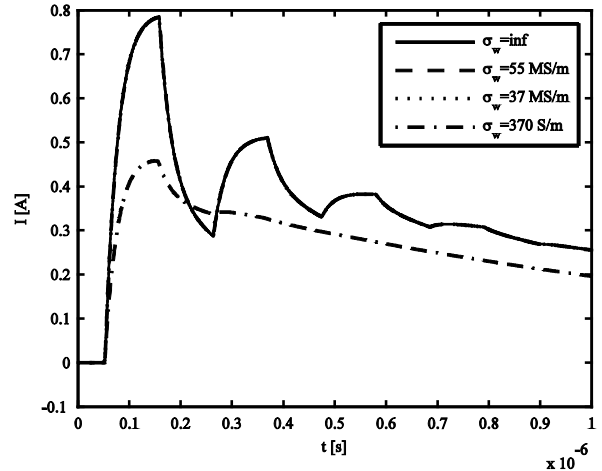


Fig. 15. Transient current at the center of the electrode, $L=10$ m, $\sigma=1$ mS/m, $0.1/1 \mu\text{s}$ pulse.

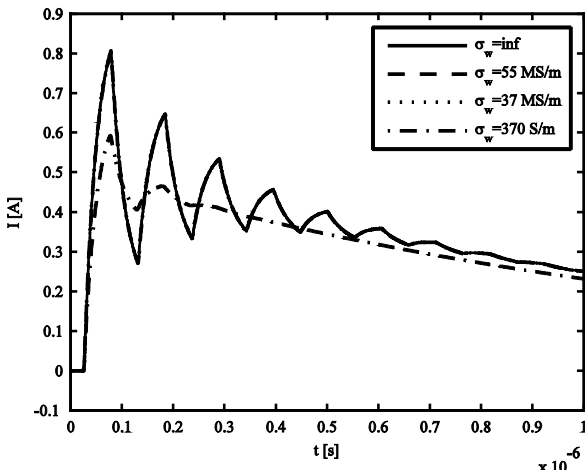


Fig. 13. Transient current at the center of the electrode, $L=5$ m, $\sigma=1$ mS/m, $0.1/1 \mu\text{s}$ pulse.

Considering the results shown in Figures 2 - 15, it can be concluded that the approximation of the perfectly conducting grounding electrode is an acceptable one when dealing with the calculation of the induced current distribution along the electrode as well as the transient response. Incorporating finite conductivity of the electrode in the electromagnetic model makes the model more complex while not improving its accuracy.

V. CONCLUSION

In this paper, the influence of the finite conductivity of the grounding electrode to the frequency and time domain analysis of the current distribution has been investigated. The governing Pocklington integro-differential equation for the induced current is posed in the frequency domain. The solution is undertaken analytically and is subsequently transformed in the time domain using IFFT. The electrode conductivity is taken into account via the concept of per-unit-length impedance. The results for the frequency domain current distribution and induced transient current show the influence of the conductivity, for electrodes made of copper or aluminum, to be rather negligible.

REFERENCES

- [1] I. T. Report, "Wind Turbine Generation System – 24: Lightning Protection, TR61400-24," 2002.
- [2] B. Glushakow, "Effective Lightning Protection For Wind Turbine Generators," *IEEE Transactions on Energy Conversion*, vol. 22, no. 1, pp. 214-222, 2007.
- [3] F. Rachidi, M. Rubinstein, J. Montanya, J.-L. Bermudez, R. R. Sola, G. Sola and N. Korovkin, "A Review of Current Issues in Lightning Protection of New-Generation Wind-Turbine Blades," *IEEE Transactions on Industrial Electronics*, vol. 55, no. 6, pp. 2489-2496, 2008.
- [4] L. Grcev and F. Dawalibi, "An electromagnetic model for transients in grounding systems," *IEEE Transactions on Power Delivery*, vol. 5, no. 4, pp. 1773-1781, November 1990.
- [5] D. Poljak, »Calculation of the transient impedance with the proposed design of grounding system for wind turbine VEJelinak (Proračun tranzijentne impedancije (udarnogotpora) s prijedlogom izvedbe uzemljivača vjetroagregata VEJelinak),« Split, 2010.
- [6] S. M. Rao, Time Domain Electromagnetics, S. M. Rao, Ed., San Diego: Academic Press, 1999.
- [7] D. Poljak, Advanced Modeling in Computational Electromagnetic Compatibility, New Jersey: Wiley-Interscience, 2007.
- [8] M. Loeloeiaan, R. Velazquez and D. Mukhedkar, "Review Of Analytical Methods For Calculating The Performance Of Large Grounding Electrodes PART II: Numerical Results," *IEEE Transactions on Power Apparatus and Systems*, vol. 104, no. 11, pp. 3134-3141, November 1985.
- [9] S. Tkatchenko, F. Rachidi and M. Ianoz, "Electromagnetic Field Coupling to a Line of Finite Length: Theory and Fast Iterative Solutions in Frequency and Time Domains," *IEEE Transactions on Electromagnetic Compatibility*, vol. 37, no. 4, pp. 509-517, November 1995.
- [10] S. Tkatchenko, F. Rachidi and M. Ianoz, "High-Frequency Electromagnetic Field Coupling to Long Terminated Lines," *IEEE Transactions on Electromagnetic Compatibility*, vol. 43, no. 2, pp. 117-129, May 2001.
- [11] R. W. P. King, G. J. Fikioris and R. B. Mack, Cylindrical Antennas and Arrays, Cambridge: Cambridge University Press, 2002.
- [12] R. W. P. King, "Embedded Bare and Insulated Antennas," *IEEE Transactions on Biomedical Engineering*, vol. 24, no. 3, pp. 253-260, May 1977.
- [13] R. W. P. King, B. S. Tremblay and J. W. Strohbehn, "The Electromagnetic Field of an Insulated Antenna in a Conducting or Dielectric Medium," *IEEE Transactions on Microwave Theory and Techniques*, vol. 31, no. 7, pp. 574-583, July 1983.
- [14] R. W. P. King, "A Review of Analytically Determined Electric Fields and Currents Induced in the Human Body When Exposed to 50–60-Hz Electromagnetic Fields," *IEEE Transactions on Antennas and Propagation*, vol. 52, no. 5, pp. 1186-1192, May 2004.
- [15] D. Poljak, S. Sesnic and R. Goic, "Analytical versus boundary element modelling of horizontal ground electrode," *Engineering Analysis with Boundary Elements*, vol. 34, pp. 307-314, 2010.
- [16] F. M. Tesche, M. Ianoz and T. Karlsson, EMC Analysis Methods and Computational Models, New York: John Wiley & Sons, Inc., 1997.
- [17] E. J. Rothwell and M. J. Cloud, Electromagnetics, Boca Raton, London, New York, Washington, D.C.: CRC Press, 2001.
- [18] D. Poljak and V. Doric, "Wire antenna model for transient analysis of simple grounding systems, Part II: The horizontal grounding electrode," *Progress In Electromagnetics Research*, vol. 64, pp. 167-189, 2006.
- [19] E. K. Miller, "A Selective Survey of Computational Electromagnetics," *IEEE Transactions on Antennas and Propagation*, vol. 36, no. 9, pp. 1281-1305, September 1988.
- [20] J. A. Stratton, Electromagnetic Theory, New Jersey: Wiley-Interscience, 2007.
- [21] E. K. Miller, A. J. Poggio, G. J. Burke and E. S. Selden, "Analysis of wire Antennas in the Presence of a Conducting Half-Space. Part II. The Horizontal Antenna in Free Space," *Canadian Journal of Physics*, vol. 50, pp. 2614-2627, 1972.
- [22] T. Takashima, T. Nakae and R. Ishibashi, "Calculation of Complex Fields in Conducting Media," *IEEE Transactions on Electrical Insulation*, vol. 15, no. 1, pp. 1-7, February 1980.
- [23] D. Poljak and N. Kovac, "Time domain modeling of a thin wire in a two-media configuration featuring a simplified reflection/transmission coefficient approach," *Engineering Analysis with Boundary Elements*, vol. 33, pp. 283-293, 2009.
- [24] J. C. Bogerd, A. G. Tijhuis and J. J. A. Klaasen, "Electromagnetic Excitation of a Thin Wire: A Traveling-Wave Approach," *IEEE Transactions on Antennas and Propagation*, vol. 46, no. 8, pp. 1202-1211, August 1998.
- [25] S. Sesnic, D. Poljak and S. Tkachenko, "Time domain analytical modeling of a straight thin wire buried in a lossy medium," *Progress In Electromagnetics Research*, vol. 121, pp. 485-504, 2011.



Silvestar Šesnić was born in Split, Croatia in 1979. He received the B.Sc. and Ph.D. degrees in electrical engineering from the University of Split, Split, Croatia in 2002 and 2010, respectively. He also received M.Phil. degree in environmental electromagnetic compatibility from the University of Wales, UK in 2005.



Dragan Poljak (M'96) was born in Split, Croatia, in 1965. He received the B.Sc., M.Sc., and Ph.D. degrees in electrical engineering from the University of Split, Split, Croatia, in 1990, 1994, and 1996, respectively.

He is currently a Full Professor in the Department of Electronics, University of Split, and an Adjunct Professor at the Wessex Institute of Technology, Southampton, U.K.

He has published nearly 200 journal and conference papers in the area of computational electromagnetics, seven authored books and one edited book by WIT Press, Southampton/Boston, and one book by Wiley, NJ. His research interests include frequency- and time-domain computational methods in electromagnetics, particularly in the numerical modeling of wire antenna structures, and recently numerical modeling applied to environmental aspects of electromagnetic fields.

Dr. Poljak is a member of the Editorial Board of the Journal *Engineering Analysis with Boundary Elements*, and the Co-Chairman of the WIT International Conference on Computational Methods in Electrical Engineering and Electromagnetics. He is also the Editor of the WIT Press Series *Advances in Electrical Engineering and Electromagnetics*. He has been awarded recently by the *National Prize for Science*.